

**This item is the archived peer-reviewed author-version of:**

Importance of nondiffusive transport for soil  $CO_2$  efflux in a temperate mountain grassland

**Reference:**

Roland Marilyn, Vicca Sara, Bahn Michael, Ladreiter-Knauss Thomas, Schmitt Michael, Janssens Ivan.- Importance of nondiffusive transport for soil  $CO_2$  efflux in a temperate mountain grassland  
Journal of Geophysical Research: Biogeosciences - ISSN 2169-8961 - (2015), p. 1-30  
DOI: <http://dx.doi.org/doi:10.1002/2014JG002788>

**IMPORTANCE OF NON-DIFFUSIVE TRANSPORT FOR SOIL CO<sub>2</sub> EFFLUX IN A TEMPERATE MOUNTAIN GRASSLAND**

Marilyn Roland<sup>a\*</sup>, Sara Vicca<sup>a</sup>, Michael Bahn<sup>b</sup>, Thomas Ladreiter-Knauss<sup>b</sup>, Michael Schmitt<sup>b</sup>  
and Ivan A. Janssens<sup>a</sup>

<sup>a</sup>Department of Biology, University of Antwerp, 2610 Wilrijk, Belgium

<sup>b</sup>Institute of Ecology, University of Innsbruck, 6020 Innsbruck, Austria

\*corresponding author: Marilyn Roland

Address: Room C0.15, Universiteitsplein 1, 2610 Wilrijk, Belgium

Telephone: +3232652272, Fax: +3232652271

Email: marilyn.roland@uantwerpen.be

**Keywords:** soil CO<sub>2</sub> transport; diffusion; chamber measurements; solid-state sensors; flux-gradient approach; pressure pumping

## 1 **Abstract**

2 Soil respiration and its biotic and abiotic drivers have been an important research topic in  
3 recent years. While the bulk of these efforts has focused on the emission of CO<sub>2</sub> from soils,  
4 the production and subsequent transport of CO<sub>2</sub> from soil to atmosphere received far less  
5 attention. However, to understand processes underlying emissions of CO<sub>2</sub> from terrestrial  
6 ecosystems, both processes need to be fully evaluated. In this study, we tested to what extent  
7 the transport of CO<sub>2</sub> in a grassland site in the Austrian Alps could be modelled based on the  
8 common assumption that diffusion is the main transport mechanism for trace gases in soils.  
9 Therefore, we compared the CO<sub>2</sub> efflux calculated from the soil CO<sub>2</sub> concentration gradient  
10 with the CO<sub>2</sub> efflux from chamber measurements. We used four commonly-used diffusion-  
11 driven models for the flux-gradient approach. Models generally underestimated the soil  
12 chamber effluxes and their amplitudes, indicating that processes other than diffusion were  
13 responsible for the transport of CO<sub>2</sub>. We further observed that transport rates correlated well  
14 with irradiation and, below a soil moisture content of 33%, with wind speed. This suggests  
15 that mechanisms such as bulk soil air transport, due to pressure pumping or thermal  
16 expansion of soil air due to local surface heating, considerably influence soil CO<sub>2</sub> transport at  
17 this site. Our results suggest that non-diffusive transport may be an important mechanism  
18 influencing diel and day-to-day dynamics of soil CO<sub>2</sub> emissions, leading to a significant  
19 mismatch (10-87% depending on the model used) between the two approaches at short  
20 timescales.

## 21 **1. Introduction**

22 Soil CO<sub>2</sub> efflux is the largest source of CO<sub>2</sub> from terrestrial ecosystems; annually,  
23 approximately 98 Pg CO<sub>2</sub> is emitted from soils (Bond-Lamberty and Thomson, 2010). Although  
24 in recent years the number of studies on soil CO<sub>2</sub> fluxes has increased largely, and high  
25 frequency measurements have provided new insights in short-term dynamics of CO<sub>2</sub> efflux  
26 (see e.g., Vargas et al., 2011), the efflux of CO<sub>2</sub> from soil to atmosphere and its biotic and  
27 abiotic drivers remain an important topic of debate (e.g., Subke and Bahn, 2010). A major  
28 reason for this ambiguity is related to the fact that, in the short-term, soil CO<sub>2</sub> efflux does not  
29 equal soil CO<sub>2</sub> production (also termed soil respiration, the sum of microbial and root  
30 respiration). Our limited knowledge of the CO<sub>2</sub> transport through the soil restricts our  
31 understanding of the role of the various abiotic and biotic controls on soil respiration (Phillips  
32 et al., 2011; Subke and Bahn, 2010).

33 Most often, soil CO<sub>2</sub> efflux is measured using soil chambers, but since the early 2000s, solid-  
34 state CO<sub>2</sub> sensors that measure soil CO<sub>2</sub> concentrations at different soil depths are becoming  
35 more common. In contrast to soil chambers, solid-state CO<sub>2</sub> sensors allow continuous high  
36 frequency measurements of the CO<sub>2</sub> gradient with minimal disturbance of the natural  
37 conditions, such as, air pressure or wind velocity (Pingingtha et al., 2010; Tang et al., 2003) and  
38 soil microclimate. For this reason, estimation of the soil CO<sub>2</sub> efflux from soil CO<sub>2</sub>  
39 concentrations, the so-called flux-gradient approach (or FGA), is rapidly gaining popularity  
40 (e.g., Hirano et al., 2003; Jassal et al., 2005; Jassal et al., 2004; Pumpanen et al., 2008; Tang et  
41 al., 2003; Tang et al., 2005; Turcu et al., 2005; Vargas and Allen, 2008a; Vargas and Allen,  
42 2008b). This method uses Fick's law of diffusion (Eq. 1) to compute soil CO<sub>2</sub> efflux and thus  
43 implies the assumption that diffusion is the only transport mechanism for CO<sub>2</sub> through the

44 soil. Potential effects of, for example, air pressure differences (following advection or wind  
45 shear) are often neglected. Soil CO<sub>2</sub> efflux  $F$  is calculated via the flux-gradient method as:

$$46 \quad F = -D_s \frac{\partial C}{\partial z} \quad (\text{Eq. 1});$$

47 where  $D_s$  is the effective diffusion coefficient (see Materials and Methods for more detailed  
48 information) and  $C$  is the CO<sub>2</sub> concentration at depth  $z$  in the soil.

49 Gas diffusion in soils differs from that in free air, because solid and liquid obstacles reduce  
50 the cross-sectional area and increase the mean path length for the diffusing molecules (Sallam  
51 et al., 1984; Werner et al., 2004). Soil properties such as water content, texture and bulk  
52 density therefore determine the rate of diffusion (Moldrup et al., 1999; Pumpanen et al.,  
53 2003; Vargas et al., 2010). Reliable estimates for the diffusion coefficient are of critical  
54 importance when using Fick's law to estimate soil CO<sub>2</sub> efflux from soil CO<sub>2</sub> concentrations.  
55 Several commonly used models have been proposed to calculate the diffusion coefficient, all  
56 of them depending primarily on the air-filled pore space and thus varying inversely with soil  
57 water content (Jassal et al., 2005).

58 Generally it is assumed that, provided a good estimate of the diffusion coefficient is available,  
59 the soil CO<sub>2</sub> concentration gradient translates directly to soil CO<sub>2</sub> efflux. However, there is  
60 limited evidence that non-diffusive transport, such as pressure pumping (summarized in Takle  
61 et al., 2004) and advective transport due to heating of the soil surface (Ganot et al., 2014),  
62 may strongly influence soil CO<sub>2</sub> emissions at the timescale of seconds. Air pressure at the soil  
63 surface fluctuates whenever turbulent air moves over the surface and enhances the exchange  
64 of gases at shallow depths (Kimball and Lemon, 1971). This bulk air gas transport is increased  
65 with increasing permeability of the soil, corresponding to a decreasing soil water content, and  
66 by thermal advection. As the soil water content decreases, the air-filled porosity increases,  
67 enhancing both diffusive and non-diffusive transport.

68 While the potential relevance of non-diffusive transport has been addressed at a very short  
69 timescale mostly, it is important to test if it plays a role at half-hourly time steps, which is the  
70 highest time-resolution typically achieved in soil respiration studies. So far, few such studies  
71 have tested how well rates of chamber-measured soil CO<sub>2</sub> efflux and those estimated from  
72 the flux gradient approach compare across the season (Riveros-Iregui et al., 2008), when non-  
73 diffusive transport may intermittently decouple fluxes derived from these two approaches.  
74 We aim to deduce the importance of non-diffusive transport for soil CO<sub>2</sub> effluxes by  
75 comparing two in-situ measurement methods (chamber and soil concentration gradient).  
76 Given that the CO<sub>2</sub> efflux is derived from the concentration gradient using diffusion models,  
77 the discrepancy between CO<sub>2</sub> effluxes from both measurements can be an indication for non-  
78 diffusive gas transport.  
79 We tested the hypotheses that the role of non-diffusive transport (i.e. the mismatch between  
80 the two approaches) increases with increasing radiation and wind speed and with decreasing  
81 soil moisture.

82

## 83 **2. Materials and methods**

### 84 *2. 1. Site description*

85 The study was carried out in a mountain meadow at Kaserstattalm, Neustift, in the Austrian  
86 Central Alps (cf. Bahn et al., 2009). Mean annual temperature and precipitation are 3.0 °C and  
87 1097 mm, respectively. The meadow is located at 1820 m asl and is fertilized with manure in  
88 spring, cut once in late July or early August and lightly grazed in September. The dominating  
89 plant species include the grasses *Anthoxanthum odoratum* L. and *Festuca rubra* L., and the  
90 forbs *Alchemilla vulgaris* L., *Leontodon hispidus* L. and *Trifolium repens* L. The soil is a cambisol  
91 on siliceous bedrock with a topsoil pH of 5.5. The soil texture is 43% sand, 47% silt and 11%

92 clay, the bulk density is 860 kg m<sup>-3</sup>. The meadow is characterized by a comparatively high  
93 productivity and high soil respiration rates, typical for non water-limited Central European  
94 mountain meadows (Bahn et al., 2010; Schmitt et al., 2010).

95

## 96 *2. 2. Measurements*

97 Soil CO<sub>2</sub> concentration measurements were made during the growing season of 2009 using  
98 Vaisala CARBOCAP solid-state CO<sub>2</sub> sensors (model GMT 221, Vaisala, Helsinki, Finland) at  
99 depths of 10 and 5 cm and the Li-8150 system (Li-Cor, Lincoln, NE, USA) at 0 cm. At the same  
100 depths, soil temperature (averaging soil thermocouple probe TCAV; Campbell Scientific) and  
101 moisture (ML2x; Delta-T Devices, Cambridge, UK) were measured, and incident  
102 photosynthetically active radiation (PAR) (BF2H; Delta-T Devices) was measured above the  
103 canopy at 2m height. Continuous recordings at 0.05 Hz were averaged and half-hourly values  
104 recorded using an automated station (CR10X; Campbell Scientific). Values of soil CO<sub>2</sub>  
105 concentration were corrected for temperature and pressure using the ideal gas law according  
106 to the manufacturer (Vaisala, Helsinki, Finland). Soil CO<sub>2</sub> efflux at the soil surface was  
107 measured using an automated soil respiration system (Li-8100 and Li-8150; Li-Cor, Lincoln,  
108 NE, USA) over measurement intervals of 2 minutes. The chambers were white to minimize  
109 heating. Possible pressure changes due to a Venturi effect are largely eliminated by the  
110 design of the vent used with the chamber (Xu et al., 2006).

111

## 112 *2. 3. CO<sub>2</sub> diffusion through the soil*

### 113 *2.3.1 Effective diffusivity*

114 Using Fick's law (Eq. 1) to calculate soil CO<sub>2</sub> efflux from the soil CO<sub>2</sub> concentration gradient  
 115 requires good estimates of the diffusion coefficient  $D_s$  (m<sup>2</sup> s<sup>-1</sup>), also named effective  
 116 diffusivity.  $D_s$  can be estimated as

$$117 \quad D_s = D_a \xi \quad (\text{Eq. 2});$$

118 where  $D_a$  (m<sup>2</sup> s<sup>-1</sup>) is the CO<sub>2</sub> diffusion coefficient in free air and  $\xi$  (m<sup>3</sup> m<sup>-3</sup>) is the so-called  
 119 tortuosity factor, the product of the air-filled porosity  $\varepsilon_a$  and the tortuosity  $\tau$  (Jassal et al.,  
 120 2005; Jury et al., 1991). It accounts for the increase in path length and decrease in cross-  
 121 sectional area in soils.

122 The variation of  $D_a$  with temperature and pressure is given by

$$123 \quad D_a = D_{a0} \left( \frac{T}{T_0} \right)^{1.75} \left( \frac{P}{P_0} \right) \quad (\text{Eq. 3});$$

124 with  $T$  the temperature (K),  $P$  the air pressure (Pa) and  $D_{a0}$  a reference value at  $T_0$  (293.15 K)  
 125 and  $P_0$  (1.013 × 10<sup>5</sup> Pa), given as 1.47 × 10<sup>-5</sup> m<sup>2</sup>s<sup>-1</sup> (Jones, 1992).

126

127 The air-filled pore space  $\varepsilon_a$  (m<sup>3</sup> m<sup>-3</sup>) is defined as the difference between total porosity  $\phi$  and  
 128 the volumetric water content  $\theta$  (m<sup>3</sup> m<sup>-3</sup>) of the soil.

$$129 \quad \varepsilon_a = \phi - \theta \quad (\text{Eq. 4}).$$

130 Several relationships between  $\xi$  and  $\varepsilon_a$  have been proposed to determine the adjustment  
 131 factor  $\xi$ . Here we compare four of the most commonly used models.

$$132 \quad \xi = 0.66 \varepsilon_a \quad (\text{Penman, 1940}) \quad (\text{Eq. 5})$$

$$133 \quad \xi = \varepsilon_a^{1.5} \quad (\text{Marshall, 1959}) \quad (\text{Eq. 6})$$

$$134 \quad \xi = \frac{\varepsilon_a^{10/3}}{\phi^2} \quad (\text{Millington and Quirk, 1961}) \quad (\text{Eq. 7})$$

$$135 \quad \xi = \phi^2 \left( \frac{\varepsilon_a}{\phi} \right)^{\beta S} \quad (\text{Moldrup et al., 1999}) \quad (\text{Eq. 8})$$

136 In Eq. 8,  $S$  is the percentage of mineral soil with particle size  $> 2 \mu\text{m}$  ( $S = 0.8$  for our study site)  
137 and  $\beta$  is a constant equal to 2.9. Total porosity at the site is  $0.57 \text{ m}^3 \text{ m}^{-3}$ . Note that in all four  
138 models, the air-filled pore space and thus total porosity, is a key factor determining the  
139 calculated efflux. Measurements of porosity on soil cores are often subject to uncertainties,  
140 especially on heterogeneous soils, and 10% uncertainty in estimated porosity translates into  
141 27-80% uncertainty in calculated efflux (depending on the model used). For this uncertainty,  
142 corresponding to a porosity range of 0.51 to  $0.63 \text{ m}^3 \text{ m}^{-3}$  at our study site, the Millington and  
143 Quirk (1961) model is the most sensitive (up to 80% uncertainty on the efflux), while the  
144 Penman (1940) model is the least sensitive (27% uncertainty on the efflux).

145

### 146 *2.3.2 Apparent diffusivity, $D_{app}$*

147 The combination of chamber measurements and solid-state sensors allows calculation of the  
148 diffusion coefficient solely from measurements. To make a distinction with the effective  
149 diffusivities  $D_s$  calculated from Eqs. 5-8, we refer to the empirically obtained diffusivity  
150 coefficient as “apparent diffusivity,  $D_{app}$ ”. To calculate this, we used the difference between  
151 the  $\text{CO}_2$  concentration measurements at 5 and 0 cm depth, which should capture the most  
152 productive zone of the grassland rhizosphere. When calculating  $D_{app}$  from Fick’s law (Eq. 1), it  
153 is necessary to account for the temperature gradient in the soil, that causes changes in the  
154 soil air density and thus in the absolute gas concentration (Kowalski and Argueso, 2011).  
155 When this concentration gradient is proportional to the gradient in air density, it will not  
156 result in diffusional transport and yield wrong fluxes. Therefore we expressed  $\text{CO}_2$   
157 concentration as a molar fraction and accounted for the air density.

158

$$F = -\rho D_s \frac{\partial C}{\partial z} \quad (\text{Eq. 9});$$

159 where  $F$  is the mass flux ( $\text{kg m}^{-2} \text{s}^{-1}$ ),  $\rho$  is the density of air ( $\text{kg m}^{-3}$ )  $C$  is the relative  $\text{CO}_2$   
160 concentration (dimensionless) at depth  $z$  (m) in the soil.

161  $D_{app}$  can then be calculated by rearranging this equation:

$$162 \quad D_{app} = -F_{ch} \frac{\partial z}{\rho \partial C} \text{ (Eq. 10);}$$

163 It is important to note that if the chamber soil  $\text{CO}_2$  efflux results from transport mechanisms  
164 other than diffusion, these are also comprised by  $D_{app}$ .

165

### 166 **3. Results**

#### 167 *3.1 Measurements of soil $\text{CO}_2$ concentrations and soil $\text{CO}_2$ efflux*

168 Chamber-based measurements of soil  $\text{CO}_2$  efflux showed most variability at daily timescales,  
169 with an amplitude apparently in phase with variations in temperature, light (PAR) and wind  
170 speed (Fig. 1). Soil  $\text{CO}_2$  concentrations measured with solid state sensors at 5 cm and 10 cm  
171 depth and measured with the Li-8150 system at 0 cm depth, were much less variable, both at  
172 seasonal and daily timescales. As the  $\text{CO}_2$  gradient is a driver of the  $\text{CO}_2$  efflux, we expected a  
173 clear relationship between the two types of measurements, but we found that the soil  $\text{CO}_2$   
174 concentration gradients from 5 to 0 cm and from 10 to 5 cm depth were uncoupled from the  
175 efflux measured with the chambers. Slopes of the correlations between the concentration  
176 measurements at 10 cm and at 5 cm depth with the fluxes, were not significantly different  
177 from zero ( $p=0.92$  and  $p=0.33$  respectively).

178

#### 179 *3.2 Calculation of soil $\text{CO}_2$ efflux with flux-gradient approach*

180 Using Fick's law (Eq. 1), we calculated the soil  $\text{CO}_2$  efflux from the measured soil  $\text{CO}_2$   
181 concentrations at 5 and 0 cm depth and the modeled diffusivity. We will refer to this  
182 calculated flux as the solid-state  $\text{CO}_2$  efflux, as distinct from the chamber  $\text{CO}_2$  efflux. Note that

183 we did not use the concentrations at 10 cm depth in this analysis, as the peak rhizosphere  
184 activity is assumed to be in the upper 5 cm of the soil. The four different models (see Eq. 5-8)  
185 to estimate the effective diffusivity,  $D_s$ , revealed large differences in estimated soil CO<sub>2</sub> efflux.  
186 Using the Penman (1940) and Marshall (1959) models for  $D_s$  yielded flux estimates within the  
187 range of the chamber measured fluxes, while the Moldrup et al. (1999) and Millington and  
188 Quirk (1961) models for  $D_s$  were both considerably lower than the chamber CO<sub>2</sub> effluxes (Fig.  
189 2). Importantly, none of the four models was able to reproduce the large daily variation in soil  
190 CO<sub>2</sub> efflux that was observed with the chamber-based measurements (Fig. 2).  
191 The diurnal course of the solid-state fluxes clearly followed that of the CO<sub>2</sub> concentrations,  
192 soil temperature and soil moisture content, while the course of the chamber fluxes followed  
193 that of wind speed and PAR. As a result, the daily peaks of solid-state fluxes lagged the  
194 chamber fluxes with approximately 4 hours.

195

### 196 *3.3 Effective and apparent diffusivity, $D_s$ and $D_{app}$*

197 By inverting Fick's law and combining the chamber-based CO<sub>2</sub> efflux measurements and the  
198 solid-state CO<sub>2</sub> concentration measurements, we calculated  $D_{app}$  and compared this with the  
199 four commonly used models to calculate  $D_s$ .  $D_s$  calculated from all four models differed  
200 strongly from  $D_{app}$  (Fig. 3a). While  $D_s$  decreases linearly with increasing soil moisture,  $D_{app}$   
201 revealed a different pattern (Fig. 3a). Only for soil water contents above 33%,  $D_{app}$  decreased  
202 markedly with increasing soil moisture. At soil water contents below 33%,  $D_{app}$  was unrelated  
203 to soil moisture and varied substantially even at similar values of soil water content.  
204 Because soil moisture is the primary determinant of gas diffusion in soils (see Eq. 4-8), the  
205 high variation of  $D_{app}$  at similar soil moisture, especially at soil moisture levels below 33%,  
206 suggests that processes other than diffusion influence the transport of CO<sub>2</sub> from soil to

207 atmosphere. Therefore, we tested whether light (PAR), soil temperature and wind speed  
208 affected  $D_{app}$ . Fig. 3b and 3c show that  $D_{app}$  indeed responded positively to variations in light  
209 and wind speed. We found no correlation between the soil temperature and  $D_{app}$  and also the  
210 temperature dependence of  $D_s$  was very weak (data not shown). We further explored the  
211 correlations of  $D_{app}$  with light and wind speed by fitting for each day the 48 half-hourly values  
212 of  $D_{app}$  versus PAR and wind speed. The correlation of  $D_{app}$  and wind speed was consistently  
213 positive for days with relatively low soil water content (<33%; Fig. 4a, asterisks). Correlations  
214 between  $D_{app}$  and PAR were positive for almost all days (Fig. 4b), indicating that  $D_{app}$  and thus  
215 the rate of  $CO_2$  transport, increases with higher irradiation. Furthermore, the slopes of the  
216 24-hour fits of  $D_{app}$  versus PAR were positively correlated with wind speed (Fig. 4c), indicating  
217 that the coupling of  $D_{app}$  and irradiation is amplified under windy conditions. To rule out any  
218 bias in either of our field measurement series, we subjected other datasets of combined solid-  
219 state and chamber measurements, from the previous year and with different placement, to  
220 this analysis and found similar results (data not shown).

221 We tested how much of the overall variation in  $D_{app}$  could be attributed to variation in PAR,  
222 wind speed and soil moisture, both for days above and below the threshold of 33% soil  
223 moisture content. The results of these multiple linear regressions are summarized in Table 1.  
224 For the entire dataset, the combination of the three parameters explained 67% of the  
225 variation in  $D_{app}$ . The combination of wind speed and PAR explained a larger part of the  
226 variation in  $D_{app}$  under moderately wet conditions (47%) than under very wet conditions  
227 (40%).

228 Comparing half-hourly values of soil  $CO_2$  concentrations with soil  $CO_2$  efflux measured once  
229 every half hour, implies comparing different integration times. To avoid statistical bias related  
230 to a reduction in variability due to longer integration time, we tested how the soil  $CO_2$  efflux

231 depended on the integration time of the flux-gradient approach. To this end, we used the  
232 Penman (1940) equation, because it yielded the best result in predicting the effective  
233 diffusivity in the soil (see Fig. 2). Increasing the integration time of the solid state and chamber  
234 measurements resulted in slightly improving accordance between  $D_{app}$  and  $D_s$  (Fig. 5), but  
235 even increasing the integration time to one month yielded poor agreement between  $D_{app}$  and  
236  $D_s$ .

237

#### 238 **4. Discussion**

239 Soil CO<sub>2</sub> concentrations and effluxes were studied at a mountain meadow in the Stubai valley  
240 (Austrian Alps) during the period of peak biomass production in 2009. Diurnal variations in  
241 concentrations were small, while they were much larger for the chamber measurements,  
242 exceeding even the seasonal variability. Furthermore, when pooling all data pairs, both types  
243 of measurements seemed largely uncoupled, which is surprising given that the concentration  
244 difference of CO<sub>2</sub> between soil and atmosphere is assumed to be the main driver of the soil  
245 CO<sub>2</sub> efflux. Part of this uncoupling might be attributable to a time lag between photosynthesis  
246 and CO<sub>2</sub> efflux, as reported by Vargas et al. (2011), but since such lag was not observed in the  
247 times series of soil CO<sub>2</sub> concentration and efflux (Fig. 1), we expect it to play a minor role here.  
248 The importance of a storage term was evaluated by looking at the instantaneous changes in  
249 soil CO<sub>2</sub> concentrations, but as these turned out to be very small, a storage flux is unlikely to  
250 explain the uncoupling of concentration and flux measurements here. Flechard et al. (2007)  
251 pointed out that storage occurs only when diffusive transport prevails.

252 To evaluate the importance of non-diffusive transport mechanisms in determining the soil  
253 CO<sub>2</sub> efflux at this site, we compared solid-state CO<sub>2</sub> fluxes, calculated with the flux-gradient  
254 approach, to the chamber CO<sub>2</sub> fluxes. The use of Fick's law in the flux-gradient approach

255 requires estimates of soil diffusivity that are in turn determined by the tortuosity factor.  
256 Different models exist for calculation of this tortuosity factor, all of them depending strongly  
257 on the air-filled pore space and thus on the soil water content (Werner et al., 2004). Among  
258 the models tested here, the Penman (1940) and Marshall (1959) models performed better  
259 with respect to the overall magnitude of the flux, the Penman model also being the least  
260 sensitive to uncertainties in porosity estimates. The Penman model yielded the highest soil  
261 CO<sub>2</sub> effluxes, which, in contrast to what has been frequently reported (Pingingtha et al., 2010;  
262 Sallam et al., 1984; Werner et al., 2004), did not exceed chamber fluxes, but predicted fluxes  
263 within the same range. The other three models resulted in fluxes (much) lower than those  
264 from chamber measurements. This was especially the case for the Moldrup et al. (1999) and  
265 Millington and Quirk (1961) model, although these have often been reported as yielding the  
266 best results (Pingingtha et al., 2010; Sallam et al., 1984; Werner et al., 2004). In our study, the  
267 most important outcome was that none of these diffusivity models was able to predict the  
268 short term (i.e. diel and day to day) variation of the soil CO<sub>2</sub> efflux in an acceptable way (Fig.  
269 2).

270 Further analyses pointed out that this disagreement is related to the fact that the tortuosity  
271 models, based on diffusive transport, depend almost completely on the soil water content.  
272 The role of the moisture content on diffusive transport is twofold. First, by decreasing the air-  
273 filled pore space, as diffusion of CO<sub>2</sub> through water is much slower than diffusion through air.  
274 Second, there can be a hysteric effect of the water content on the effective diffusivity,  $D_s$   
275 being higher at a similar water content during wetting than during drying (Goffin et al., 2014;  
276 Rouf et al., 2012). It is important to note here that also the short-term response of soil  
277 respiration to changes in soil moisture is not monotonic; CO<sub>2</sub> production increases from low

278 to intermediate soil moisture, reaches a plateau at optimum moisture, and decreases again  
279 at high soil moisture (Vicca et al., 2014).

280 At our site, however, the rate of CO<sub>2</sub> transport from soil to atmosphere depended not only  
281 on soil moisture, but also on irradiation (PAR) and wind speed. Correlation coefficients of the  
282 fits of apparent diffusivity,  $D_{app}$ , versus wind speed were consistently positive on days that  
283 were not very wet, i.e. when soil water content was below 33% (Fig. 4a).  $D_{app}$  was also  
284 positively related to PAR (Fig. 4b), indicating a positive light effect on CO<sub>2</sub> transport from soil  
285 to atmosphere. Last, the slopes of the linear regressions showed that the coupling of  $D_{app}$  and  
286 PAR became stronger as wind speed increased (Fig. 4c). Note that higher values of PAR and  
287 wind speed were recorded in periods when soil moisture content was below 33%, therefore  
288 leading also to higher values of  $D_{app}$  in these periods. The response of  $D_{app}$  to these drivers,  
289 on the other hand, did not differ for periods with soil moisture content above and below 33%  
290 (intercepts of the correlations differed but not the slopes). The effect of wind speed on  $D_{app}$   
291 was similar during day and night time.

292 The large diel variations we observed in  $D_{app}$  and its tight coupling to PAR, should not be  
293 mistaken for a soil respiration-driven effect on diffusive CO<sub>2</sub> transport. Soil respiration is  
294 known to be strongly influenced by temperature and thus exhibits a pronounced diel pattern.  
295 This diel pattern can be further amplified by the linkage between belowground carbon  
296 allocation and photosynthetic activity. The increase in photoassimilates allocated  
297 belowground was often shown to stimulate autotrophic and heterotrophic respiration (Bahn  
298 et al., 2009; Hogberg et al., 2001; Janssens et al., 2001; Kuzyakov, 2006; Kuzyakov and  
299 Gavrichkova, 2010).

300 The diurnal pattern in soil respiration was clearly seen in the chamber-based soil CO<sub>2</sub> efflux  
301 measurements, but surprisingly much less in the soil CO<sub>2</sub> concentration measurements. This

302 suggests that an increased transport rate, exceeding diffusion, during the day must have  
303 prevented soil CO<sub>2</sub> concentrations to rise, while soil respiration did increase. Diffusion  
304 depends primarily on soil moisture and on the concentration gradient, both of which varied  
305 only little during the day. Enhanced transport of CO<sub>2</sub> through the soil, via other processes  
306 should thus explain the discrepancy between the large diel amplitude of soil CO<sub>2</sub> efflux and  
307 the relatively steady soil CO<sub>2</sub> concentrations.

308 Several mechanisms causing bulk flow of CO<sub>2</sub>-enriched soil air have been described in  
309 literature (see Kuang et al. (2013) for an extensive review) and can occur in all soils when  
310 pores are connected and not blocked by water (Cuezva et al., 2011). An increasing number of  
311 authors have demonstrated a positive correlation between pressure pumping and soil CO<sub>2</sub>  
312 efflux (Arneeth et al., 1998; Baldocchi and Meyers, 1991; Lewicki et al., 2010; Subke et al.,  
313 2003). Takle et al. (2004) found that these pressure fluctuations penetrated into a dry soil up  
314 to 50 cm with little attenuation and Bowling and Massman (2011) found a temporarily  
315 transport enhancement through a forest snowpack up to 40% higher than diffusion. Pressure  
316 pumping is controlled by the degree of permeability of the medium and the direction and  
317 magnitude of the pressure gradient (Massman et al., 1995; Takle et al., 2003). Pressure  
318 gradients can be caused by barometric waves, passage of synoptic weather systems, short-  
319 period atmospheric turbulence and wind blowing across irregular topography (Elberling et al.,  
320 1998; Massman et al., 1997; Takle et al., 2004).

321 Bulk air transport (in this context called ventilation) was described in permeable, dry and  
322 fractured media such as karst systems, and was found to be coupled to pressure gradients as  
323 well as wind (Rey et al., 2012; Sanchez-Canete et al., 2013; Serrano-Ortiz et al., 2010).

324 The bulk exchange of gases is enhanced when drying of the soil increases the air-filled porosity  
325 and by high wind speeds (Hirsch et al., 2004; Kimball and Lemon, 1971; Maier and Schack-

326 Kirchner, 2014; Sanchez-Canete et al., 2013; Subke et al., 2003). The positive correlation that  
327 we found between  $D_{app}$  and wind under relatively dry conditions, could therefore be  
328 attributable to pressure changes caused by wind shear at the soil surface.

329 Advective bulk air transport can also be triggered by the local heating of the soil surface  
330 (Ganot et al., 2014). This heating would not be recorded by the soil temperature sensors,  
331 which were installed at 5 and 10 cm depth, but inevitably coincides with measurements of  
332 irradiation. A second light-coupled process that may amplify bulk soil air transport is the  
333 breaking of the soil boundary layer following thermal expansion and uplifting of the air at the  
334 soil-atmosphere interface.

335 Several things could improve the ability to accurately estimate  $CO_2$  efflux from vertical  
336 concentration gradients. First,  $D_s$ , and thus porosity and tortuosity, should be estimated  
337 independently, using intact soil cores (DeSutter et al., 2008; Jassal et al., 2005) or in situ field  
338 methods based on inert tracers such as radon (Risk et al., 2008), although even these methods  
339 cannot fully capture the spatial and temporal dynamics of the soil gas diffusivity (Maier and  
340 Schack-Kirchner, 2014). Next, part of the discrepancy that we observed between solid-state  
341 and chamber  $CO_2$  efflux, might be reconciled when both types of measurements are carried  
342 out with the exact same measuring frequency and interval, as the variability of solid-state  
343 concentrations with longer integration time will typically be lower otherwise. This was also  
344 brought up by Riveros-Iregui et al. (2008), stating that solid-state sensors might not capture  
345 rapid changes in soil properties and respiration, e.g. due to rainfall events. Several authors  
346 state that the efflux rates calculated from concentration gradients might be unsuited for  
347 deriving short-term fluxes, but that they could be useful for flux estimates over longer time  
348 periods (eg. Vargas et al., 2010), when the importance of non-diffusive transport decreases.  
349 However, even after integration over one month, we found that apparent diffusivity was

350 higher than effective diffusivity (Fig. 5), thus still resulting in an underestimation of soil  
351 respiration rates by the flux-gradient approach. Substantial uncertainty may furthermore  
352 arise from the assumption of a linear CO<sub>2</sub> concentration gradient in the soil (Maier and  
353 Schack-Kirchner, 2014), although Monson et al. (2006) found it a minor source of error  
354 compared to the estimations of D<sub>s</sub>. The exact measurement height of the 0 cm concentration  
355 holds a negligible error, given that the magnitude and diel variability of soil CO<sub>2</sub> above the  
356 surface is small due to the atmospheric buffer and affects the gradient only very little (Riveros-  
357 Iregui et al., 2008; and own analysis).

358 Several previous studies did find good agreements between solid-state CO<sub>2</sub> efflux and  
359 chamber CO<sub>2</sub> efflux (Jassal et al., 2005; Liang et al., 2004; Pumpanen et al., 2008; Tang et al.,  
360 2005). These studies were conducted in dense forests where, in contrast to grasslands, both  
361 light and wind have difficulty penetrating into layers close to the soil surface. This is probably  
362 why their effect on soil gas transport was insignificant. Under such diffusion-dominated  
363 conditions, the flux-gradient approach can be successfully applied to predict the soil CO<sub>2</sub>  
364 efflux.

365

## 366 **5. Conclusions and recommendations**

367 Over the last decade, research in this field has focused on the measurement of fluxes at the  
368 soil surface using a variety of chambers and micrometeorological methods. Recently the flux-  
369 gradient approach proved to be a very cost-efficient way to calculate the soil CO<sub>2</sub> efflux that  
370 minimizes soil surface perturbations and provides insights into subsurface CO<sub>2</sub> dynamics. This  
371 method uses estimates for effective diffusivity, derived from different models primarily based  
372 on the air-filled pore space. Testing four commonly used models, we found substantial

373 deviation between observed and modeled diffusivity, leading to poor predictions of the soil  
374 CO<sub>2</sub> efflux when using the flux-gradient approach at shorter timescales.

375 Gaseous diffusion is often considered as the only mechanism for CO<sub>2</sub> to move from the soil to  
376 the atmosphere, while in reality several gas transport mechanisms can be distinguished in  
377 unsaturated porous media like soils, e.g. advective mass transport and pressure pumping. We  
378 found strong evidence for such non-diffusive CO<sub>2</sub> transport at our site, given that the rate of  
379 transport was coupled to irradiation, with an even stronger coupling under increasing wind  
380 speed. Wind speed also had a direct positive effect on the efflux rate when the soil moisture  
381 content comparatively low (< 33%), resulting in higher air-filled porosity.

382 Considering the importance of alternative transport processes is a prerequisite when using  
383 solid-state CO<sub>2</sub> concentration measurements to estimate soil CO<sub>2</sub> efflux at any given site.

384 Deviation between apparent (data-based) and effective (model-based) diffusivity may be a  
385 first indication of non-diffusive gas transport. Apparent diffusivity can be evaluated by  
386 calculation from combined chamber and solid-state sensor measurements (as demonstrated  
387 here) or by direct in situ soil gas diffusivity measurements (e.g. with natural or injected  
388 <sup>222</sup>Radon as done by Risk et al. (2008) ).

389 Given that non-diffusive transport is especially important at very short timescales and its  
390 influence decreases with increasing timescale, we recommend that future studies further  
391 explore the importance of the timescale considered (high-frequency versus low-frequency  
392 data) and the effects of uncertainties in porosity on this. Combined high-frequency  
393 measurements of soil CO<sub>2</sub> concentrations and its potential physical drivers, including air  
394 pressure and friction velocity, under a wider range of soil moisture conditions, are needed to  
395 obtain a more detailed picture of the mechanisms and timescales relevant for non-diffusive  
396 transport of CO<sub>2</sub> on soils.

397

398 **Acknowledgements**

399 We thank Karin Bianchi, Mathias Gort, Verena Gruber, Alois Haslwanger and Eric Walter for  
400 their help with data collection and quality control. All data used in this work can be obtained  
401 upon request to the corresponding author. This work has been financially supported by the  
402 Austrian Science Fund (FWF P18756-B16, P22214-B17) and the European Commission (EU-  
403 projects GHG Europe FP7-ENV-2009-1-244122 and Carbo-Extreme FP7-ENV-2008-1-226701).  
404 MR received a grant from the Institute for Promotion of Innovation through Science and  
405 Technology in Flanders (IWT). SV is a post-doctoral research associate of the Fund for  
406 Scientific Research – Flanders (FWO).

## References

- Arneeth, A. et al., 1998. Environmental variables regulating soil carbon dioxide efflux following clear-cutting of a *Pinus radiata* D. Don plantation. *J. Geophys. Res.-Atmos.*, 103(D5): 5695-5705.
- Bahn, M. et al., 2010. Soil respiration at mean annual temperature predicts annual total across vegetation types and biomes. *Biogeosciences*, 7(7): 2147-2157.
- Bahn, M., Schmitt, M., Siegwolf, R., Richter, A. and Bruggemann, N., 2009. Does photosynthesis affect grassland soil-respired CO<sub>2</sub> and its carbon isotope composition on a diurnal timescale? *New Phytol.*, 182(2): 451-460.
- Baldocchi, D.D. and Meyers, T.P., 1991. Trace gas-exchange above the floor of a deciduous forest .1. Evaporation and CO<sub>2</sub> efflux. *J. Geophys. Res.-Atmos.*, 96(D4): 7271-7285.
- Bond-Lamberty, B. and Thomson, A., 2010. Temperature-associated increases in the global soil respiration record. *Nature*, 464(7288): 579-U132.
- Bowling, D.R. and Massman, W.J., 2011. Persistent wind-induced enhancement of diffusive CO<sub>2</sub> transport in a mountain forest snowpack. *J. Geophys. Res.-Biogeosci.*, 116.
- Cuezva, S. et al., 2011. Short-term CO<sub>2</sub>(g) exchange between a shallow karstic cavity and the external atmosphere during summer: Role of the surface soil layer. *Atmos. Environ.*, 45(7): 1418-1427.
- DeSutter, T.M., Sauer, T.J., Parkin, T.B. and Heitman, J.L., 2008. A subsurface, closed-loop system for soil carbon dioxide and its application to the gradient efflux approach. *Soil Sci. Soc. Am. J.*, 72(1): 126-134.
- Elberling, B., Larsen, F., Christensen, S. and Postma, D., 1998. Gas transport in a confined unsaturated zone during atmospheric pressure cycles. *Water Resour. Res.*, 34(11): 2855-2862.
- Flechard, C.R. et al., 2007. Temporal changes in soil pore space CO<sub>2</sub> concentration and storage under permanent grassland. *Agric. For. Meteorol.*, 142(1): 66-84.
- Ganot, Y., Dragila, M.I. and Weisbrod, N., 2014. Impact of thermal convection on CO<sub>2</sub> flux across the earth-atmosphere boundary in high-permeability soils. *Agric. For. Meteorol.*, 184(0): 12-24.
- Goffin, S. et al., 2014. Characterization of the soil CO<sub>2</sub> production and its carbon isotope composition in forest soil layers using the flux-gradient approach. *Agric. For. Meteorol.*, 188: 45-57.
- Hirano, T., Kim, H. and Tanaka, Y., 2003. Long-term half-hourly measurement of soil CO<sub>2</sub> concentration and soil respiration in a temperate deciduous forest. *J. Geophys. Res.-Atmos.*, 108(D20).
- Hirsch, A.I., Trumbore, S.E. and Goulden, M.L., 2004. The surface CO<sub>2</sub> gradient and pore-space storage flux in a high-porosity litter layer. *Tellus Ser. B-Chem. Phys. Meteorol.*, 56(4): 312-321.
- Hogberg, P. et al., 2001. Large-scale forest girdling shows that current photosynthesis drives soil respiration. *Nature*, 411(6839): 789-792.
- Janssens, I.A. et al., 2001. Productivity overshadows temperature in determining soil and ecosystem respiration across European forests. *Global Change Biol.*, 7(3): 269-278.
- Jassal, R. et al., 2005. Relationship between soil CO<sub>2</sub> concentrations and forest-floor CO<sub>2</sub> effluxes. *Agric. For. Meteorol.*, 130(3-4): 176-192.
- Jassal, R.S. et al., 2004. A model of the production and transport of CO<sub>2</sub> in soil: predicting soil CO<sub>2</sub> concentrations and CO<sub>2</sub> efflux from a forest floor. *Agric. For. Meteorol.*, 124(3-4): 219-236.
- Jones, H.G., 1992. *Plants and Microclimate: A Quantitative Approach to Environmental Plant Physiology*. Cambridge University Press.
- Jury, W.A., Gardner, W.R. and Gardner, W.H., 1991. *Soil physics*. J. Wiley.
- Kimball, B.A. and Lemon, E.R., 1971. Air turbulence effects upon soil gas exchange. *Soil Science Society of America Proceedings*, 35(1): 16-&.
- Kowalski, A.S. and Argueso, D., 2011. Scalar arguments of the mathematical functions defining molecular and turbulent transport of heat and mass in compressible fluids. *Tellus Ser. B-Chem. Phys. Meteorol.*, 63(5): 1059-1066.
- Kuang, X., Jiao, J.J. and Li, H., 2013. Review on airflow in unsaturated zones induced by natural forcings. *Water Resour. Res.*, 49(10): 6137-6165.

- Kuzyakov, Y., 2006. Sources of CO<sub>2</sub> efflux from soil and review of partitioning methods. *Soil Biology & Biochemistry*, 38(3): 425-448.
- Kuzyakov, Y. and Gavrichkova, O., 2010. REVIEW: Time lag between photosynthesis and carbon dioxide efflux from soil: a review of mechanisms and controls. *Global Change Biol.*, 16(12): 3386-3406.
- Lewicki, J.L., Hilley, G.E., Dobeck, L. and Spangler, L., 2010. Dynamics of CO<sub>2</sub> fluxes and concentrations during a shallow subsurface CO<sub>2</sub> release. *Environ Earth Sci*, 60(2): 285-297.
- Liang, N.S. et al., 2004. In situ comparison of four approaches to estimating soil CO<sub>2</sub> efflux in a northern larch (*Larix kaempferi* Sarg.) forest. *Agric. For. Meteorol.*, 123(1-2): 97-117.
- Maier, M. and Schack-Kirchner, H., 2014. Using the gradient method to determine soil gas flux: A review. *Agric. For. Meteorol.*, 192: 78-95.
- Marshall, T.J., 1959. The diffusion of gases through porous media. *J. Soil Sci.*, 10(1): 79-82.
- Massman, W. et al., 1995. CO<sub>2</sub> flux through a Wyoming seasonal snowpack: Diffusional and pressure pumping effects. In: K.A. Tonnessen, M.W. Williams and M. Tranter (Editors), *International Symposium on Biogeochemistry of Seasonally Snow-Covered Catchments*, at the XXI Assembly of the International-Union-of-Geodesy-and-Geophysics. *Int Assoc Hydrological Sciences*, Boulder, Co, pp. 71-79.
- Massman, W.J. et al., 1997. A model investigation of turbulence-driven pressure-pumping effects on the rate of diffusion of CO<sub>2</sub>, N<sub>2</sub>O, and CH<sub>4</sub> through layered snowpacks. *J. Geophys. Res.-Atmos.*, 102(D15): 18851-18863.
- Millington, R. and Quirk, J.P., 1961. Permeability of porous solids. *Transactions of the Faraday Society*, 57(8): 1200-&.
- Moldrup, P., Olesen, T., Yamaguchi, T., Schjonning, P. and Rolston, D.E., 1999. Modeling diffusion and reaction in soils: IX. The Buckingham-Burdine-Campbell equation for gas diffusivity in undisturbed soil. *Soil Sci.*, 164(8): 542-551.
- Monson, R.K. et al., 2006. The contribution of beneath-snow soil respiration to total ecosystem respiration in a high-elevation, subalpine forest. *Global Biogeochem. Cycles*, 20(3).
- Penman, H.L., 1940. Gas and vapour movements in the soil: I. The diffusion of vapours through porous solids. *The Journal of Agricultural Science*, 30(03): 437-462.
- Phillips, C.L., Nickerson, N., Risk, D. and Bond, B.J., 2011. Interpreting diel hysteresis between soil respiration and temperature. *Global Change Biol.*, 17(1): 515-527.
- Pingintha, N., Leclerc, M.Y., Beasley, J.P., Zhang, G.S. and Senthong, C., 2010. Assessment of the soil CO<sub>2</sub> gradient method for soil CO<sub>2</sub> efflux measurements: comparison of six models in the calculation of the relative gas diffusion coefficient. *Tellus Ser. B-Chem. Phys. Meteorol.*, 62(1): 47-58.
- Pumpanen, J., Ilvesniemi, H. and Hari, P., 2003. A process-based model for predicting soil carbon dioxide efflux and concentration. *Soil Sci. Soc. Am. J.*, 67(2): 402-413.
- Pumpanen, J. et al., 2008. Respiration in boreal forest soil as determined from carbon dioxide concentration profile. *Soil Sci. Soc. Am. J.*, 72(5): 1187-1196.
- Rey, A. et al., 2012. Wind as a main driver of the net ecosystem carbon balance of a semiarid Mediterranean steppe in the South East of Spain. *Global Change Biol.*, 18(2): 539-554.
- Risk, D., Kellman, L. and Beltrami, H., 2008. A new method for in situ soil gas diffusivity measurement and applications in the monitoring of subsurface CO<sub>2</sub> production. *J. Geophys. Res.-Biogeosci.*, 113(G2).
- Riveros-Iregui, D.A., McGlynn, B.L., Epstein, H.E. and Welsch, D.L., 2008. Interpretation and evaluation of combined measurement techniques for soil CO<sub>2</sub> efflux: Discrete surface chambers and continuous soil CO<sub>2</sub> concentration probes. *J. Geophys. Res.-Biogeosci.*, 113(G4).
- Rouf, M.A. et al., 2012. Unified measurement system with suction control for measuring hysteresis in soil-gas transport parameters. *Water Resour. Res.*, 48.
- Sallam, A., Jury, W.A. and Letey, J., 1984. Measurement of gas-diffusion coefficient under relatively low air-filled porosity. *Soil Sci. Soc. Am. J.*, 48(1): 3-6.

- Sanchez-Canete, E.P., Kowalski, A.S., Serrano-Ortiz, P., Perez-Priego, O. and Domingo, F., 2013. Deep CO<sub>2</sub> soil inhalation/exhalation induced by synoptic pressure changes and atmospheric tides in a carbonated semiarid steppe. *Biogeosciences*, 10(10): 6591-6600.
- Schmitt, M., Bahn, M., Wohlfahrt, G., Tappeiner, U. and Cernusca, A., 2010. Land use affects the net ecosystem CO<sub>2</sub> exchange and its components in mountain grasslands. *Biogeosciences*, 7(8): 2297-2309.
- Serrano-Ortiz, P. et al., 2010. Hidden, abiotic CO<sub>2</sub> flows and gaseous reservoirs in the terrestrial carbon cycle: Review and perspectives. *Agric. For. Meteorol.*, 150: 321-329.
- Subke, J.A. and Bahn, M., 2010. On the 'temperature sensitivity' of soil respiration: Can we use the immeasurable to predict the unknown? *Soil Biology & Biochemistry*, 42(9): 1653-1656.
- Subke, J.A., Reichstein, M. and Tenhunen, J.D., 2003. Explaining temporal variation in soil CO<sub>2</sub> efflux in a mature spruce forest in Southern Germany. *Soil Biology & Biochemistry*, 35(11): 1467-1483.
- Takle, E.S. et al., 2003. High-frequency pressure variations in the vicinity of a surface CO<sub>2</sub> flux chamber. *Agric. For. Meteorol.*, 114(3-4): 245-250.
- Takle, E.S. et al., 2004. Influence of high-frequency ambient pressure pumping on carbon dioxide efflux from soil. *Agric. For. Meteorol.*, 124(3-4): 193-206.
- Tang, J.W., Baldocchi, D.D., Qi, Y. and Xu, L.K., 2003. Assessing soil CO<sub>2</sub> efflux using continuous measurements of CO<sub>2</sub> profiles in soils with small solid-state sensors. *Agric. For. Meteorol.*, 118(3-4): 207-220.
- Tang, J.W., Misson, L., Gershenson, A., Cheng, W.X. and Goldstein, A.H., 2005. Continuous measurements of soil respiration with and without roots in a ponderosa pine plantation in the Sierra Nevada Mountains. *Agric. For. Meteorol.*, 132(3-4): 212-227.
- Turcu, V.E., Jones, S.B. and Or, D., 2005. Continuous soil carbon dioxide and oxygen measurements and estimation of gradient-based gaseous flux. *Vadose Zone J.*, 4(4): 1161-1169.
- Vargas, R. and Allen, M.F., 2008a. Dynamics of fine root, fungal rhizomorphs, and soil respiration in a mixed temperate forest: Integrating sensors and observations. *Vadose Zone J.*, 7(3): 1055-1064.
- Vargas, R. and Allen, M.F., 2008b. Environmental controls and the influence of vegetation type, fine roots and rhizomorphs on diel and seasonal variation in soil respiration. *New Phytol.*, 179(2): 460-471.
- Vargas, R. et al., 2010. Looking deeper into the soil: biophysical controls and seasonal lags of soil CO<sub>2</sub> production and efflux. *Ecol. Appl.*, 20(6): 1569-1582.
- Vargas, R. et al., 2011. On the multi-temporal correlation between photosynthesis and soil CO<sub>2</sub> efflux: reconciling lags and observations. *New Phytol.*, 191(4): 1006-1017.
- Vicca, S. et al., 2014. Can current moisture responses predict soil CO<sub>2</sub> efflux under altered precipitation regimes? A synthesis of manipulation experiments. *Biogeosciences*, 11(11): 2991-3013.
- Werner, D., Grathwohl, P. and Hohener, P., 2004. Review of field methods for the determination of the tortuosity and effective gas-phase diffusivity in the vadose zone. *Vadose Zone J.*, 3(4): 1240-1248.
- Xu, L.K. et al., 2006. On maintaining pressure equilibrium between a soil CO<sub>2</sub> flux chamber and the ambient air. *J. Geophys. Res.-Atmos.*, 111(D8).

## Figure legends

### Figure 1:

Time series from May 28 until August 4 2009 of half hourly measurements of (a) soil CO<sub>2</sub> concentrations at 0, 5 and 10 cm depth, (b) soil CO<sub>2</sub> efflux from automated chambers, (c) photosynthetically active radiation (PAR), (d) soil temperature at 5 and 10 cm depth, (e) soil water content and rainfall and (f) wind speed on a mountain meadow at Kaserstattalm, Neustift, Austria.

### Figure 2:

Comparison of measured and modeled soil CO<sub>2</sub> effluxes. The black line shows the soil CO<sub>2</sub> efflux measured by the soil chambers, the colored lines are the effluxes calculated using four different models: Pm: Penman (1940), MQ: Millington and Quirk (1961), Md: Moldrup et al. (1999), Ma: Marshall (1959).

### Figure 3:

(a) Apparent diffusivity ( $D_{app}$ , black dots) and modeled diffusivity ( $D_s$ , colored dots) as a function of the soil water content (SWC) at 5 cm depth. The green lines are the regression lines of  $D_{app}$  versus SWC<33% ( $y=-0.06x+5.66$ ,  $R^2=0.02$ ,  $p<0.01$ ) and  $D_{app}$  versus SWC>33% ( $y=-0.45x+18.06$ ,  $R^2=0.30$ ,  $p<0.01$ ).

(b)  $D_{app}$  as a function of photosynthetically active radiation (PAR). The green line is the regression line ( $y=0.002x+1.81$ ,  $R^2=0.35$ ,  $p<0.01$ ).

(c)  $D_{app}$  as a function of wind speed. The green line is the regression line ( $y=0.66x+1.46$ ,  $R^2=0.10$ ,  $p<0.01$ ).

Figure 4:

(a) Correlation coefficients of 24-hour fits (using 48 half-hourly values for each fit) of apparent diffusivity ( $D_{app}$ ) and wind speed. Open circles are days with soil water content below 33%, full circles are days with soil water content above 33%.

(b) Correlation coefficients of 24-hour fits of  $D_{app}$  and of photosynthetically active radiation (PAR).

(c) Slopes of 24-hour fits of  $D_{app}$  and PAR plotted against wind speed. The black line is the regression line ( $y=0.19x+0.02$ ,  $R^2=0.15$ ,  $p<0.01$ ).

Figure 5:

The accordance between  $D_s$  (using the Penman 1940 model) and  $D_{app}$ , with increasing integration times of solid state and chamber measurements: 2 hours, 8 hours, 24 hours, 1 week and 1 month.

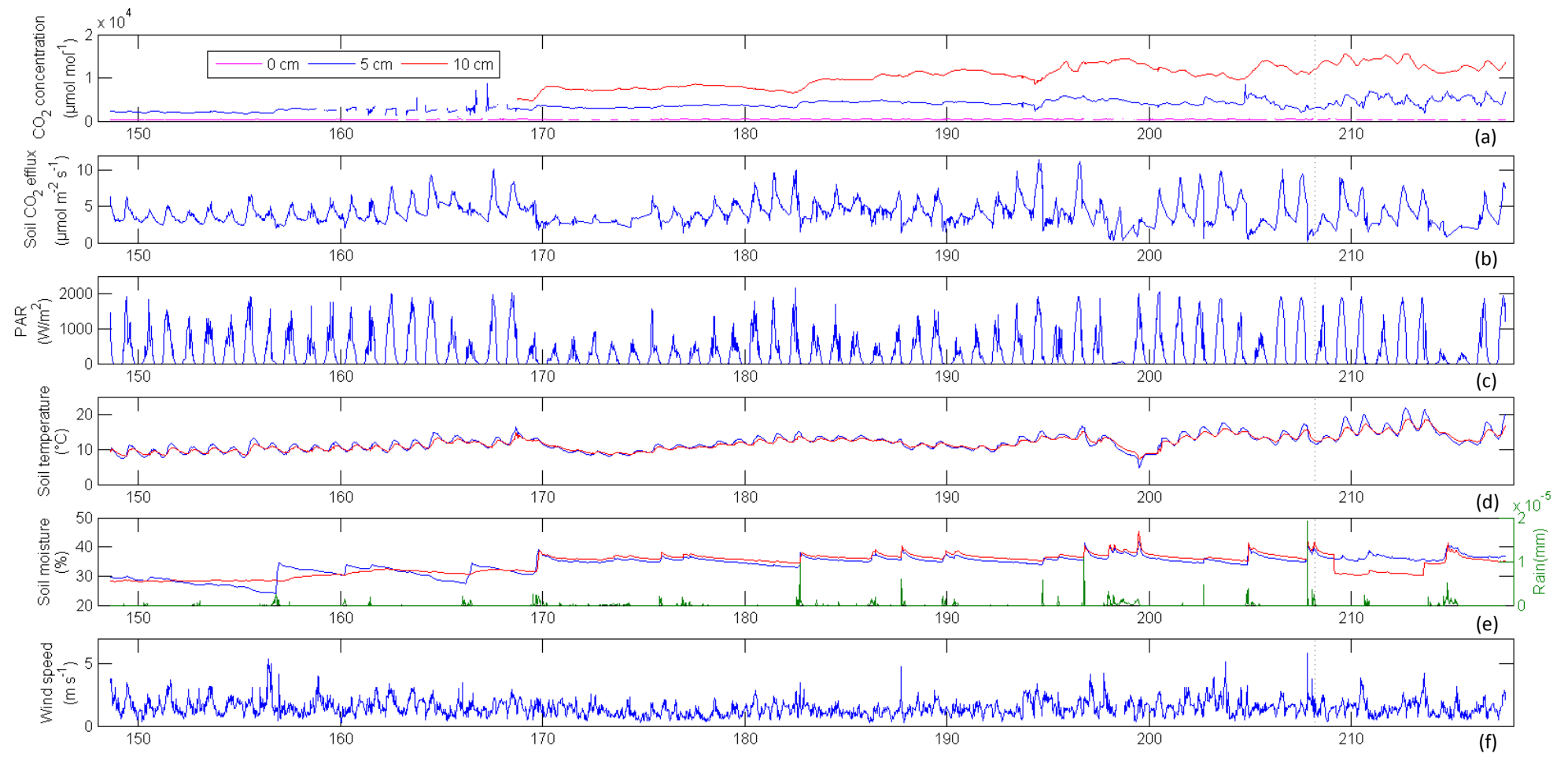


Figure 1

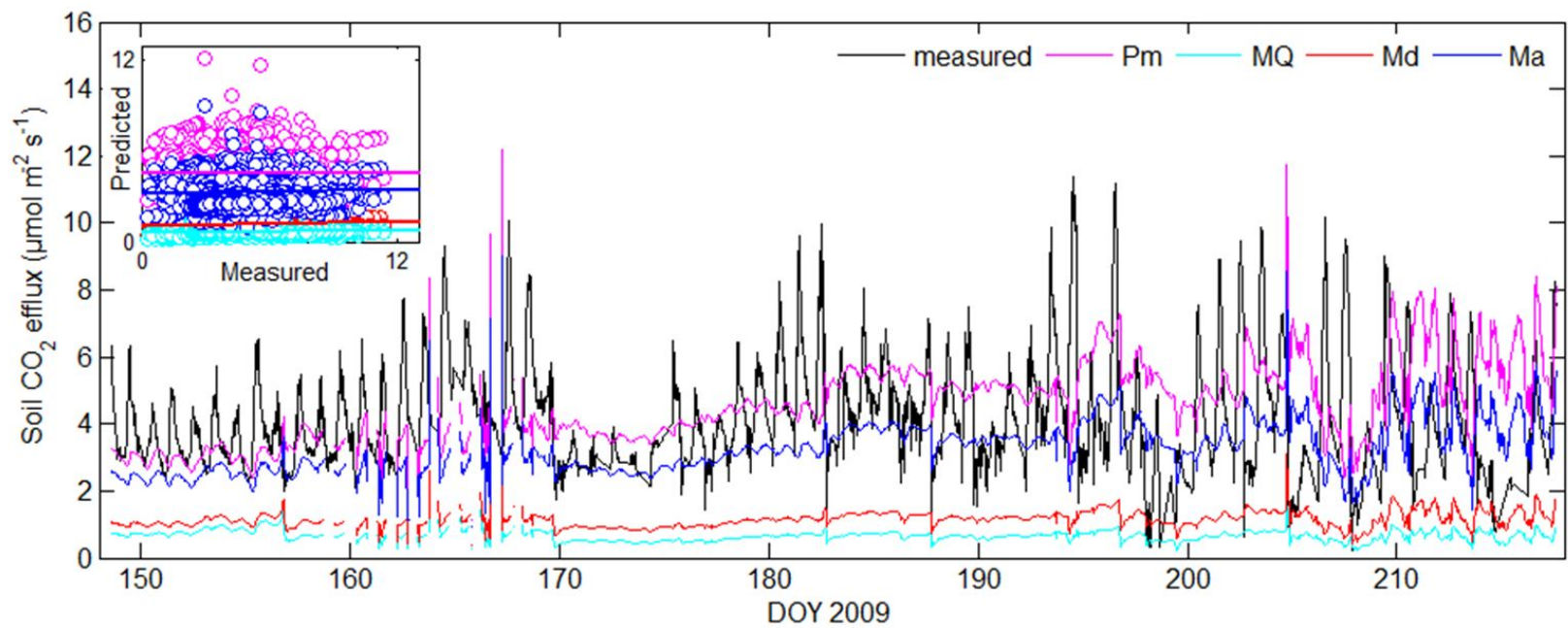


Figure 2

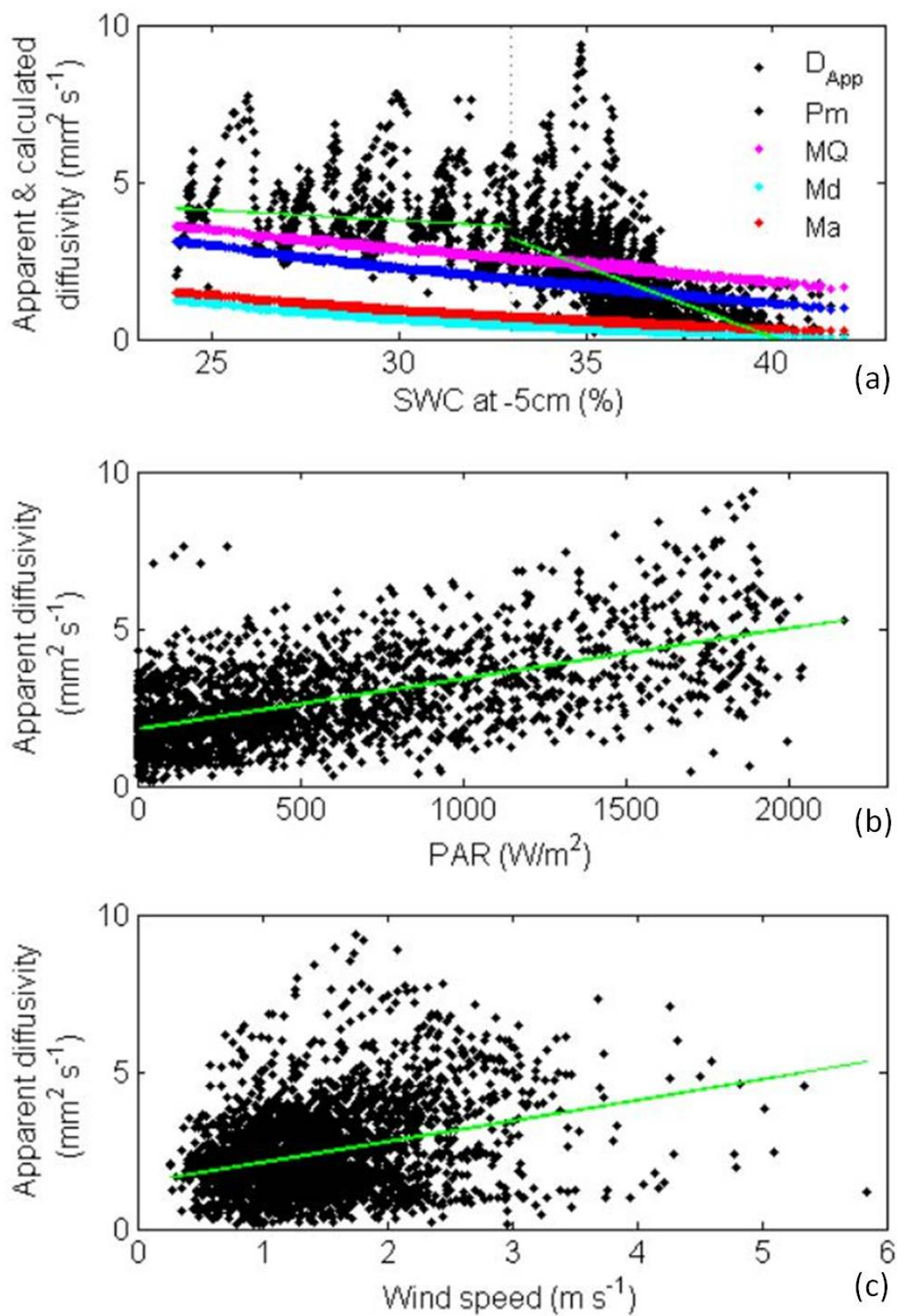


Figure 3

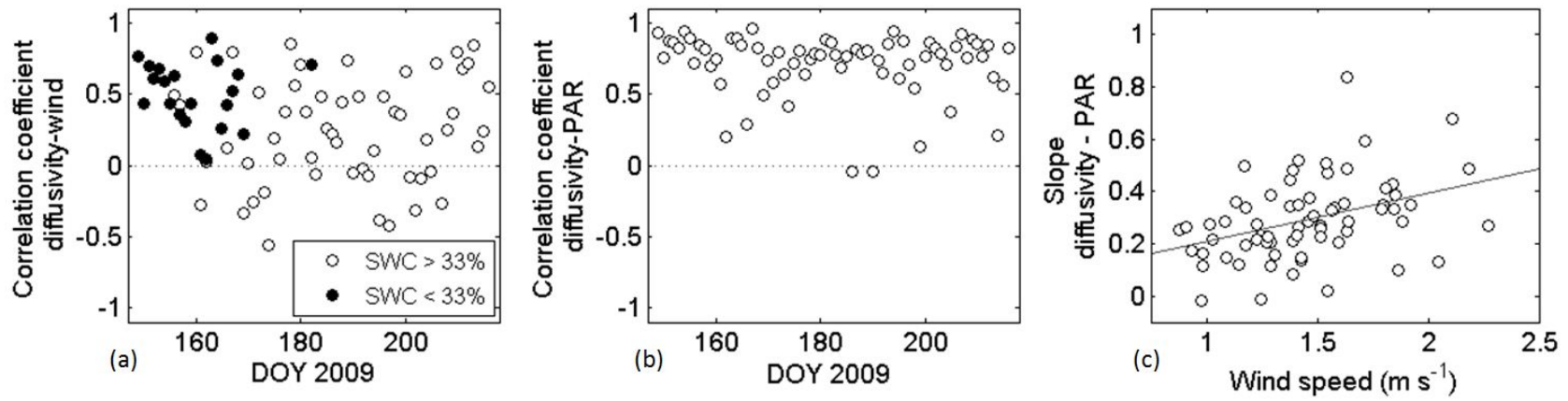


Figure 4

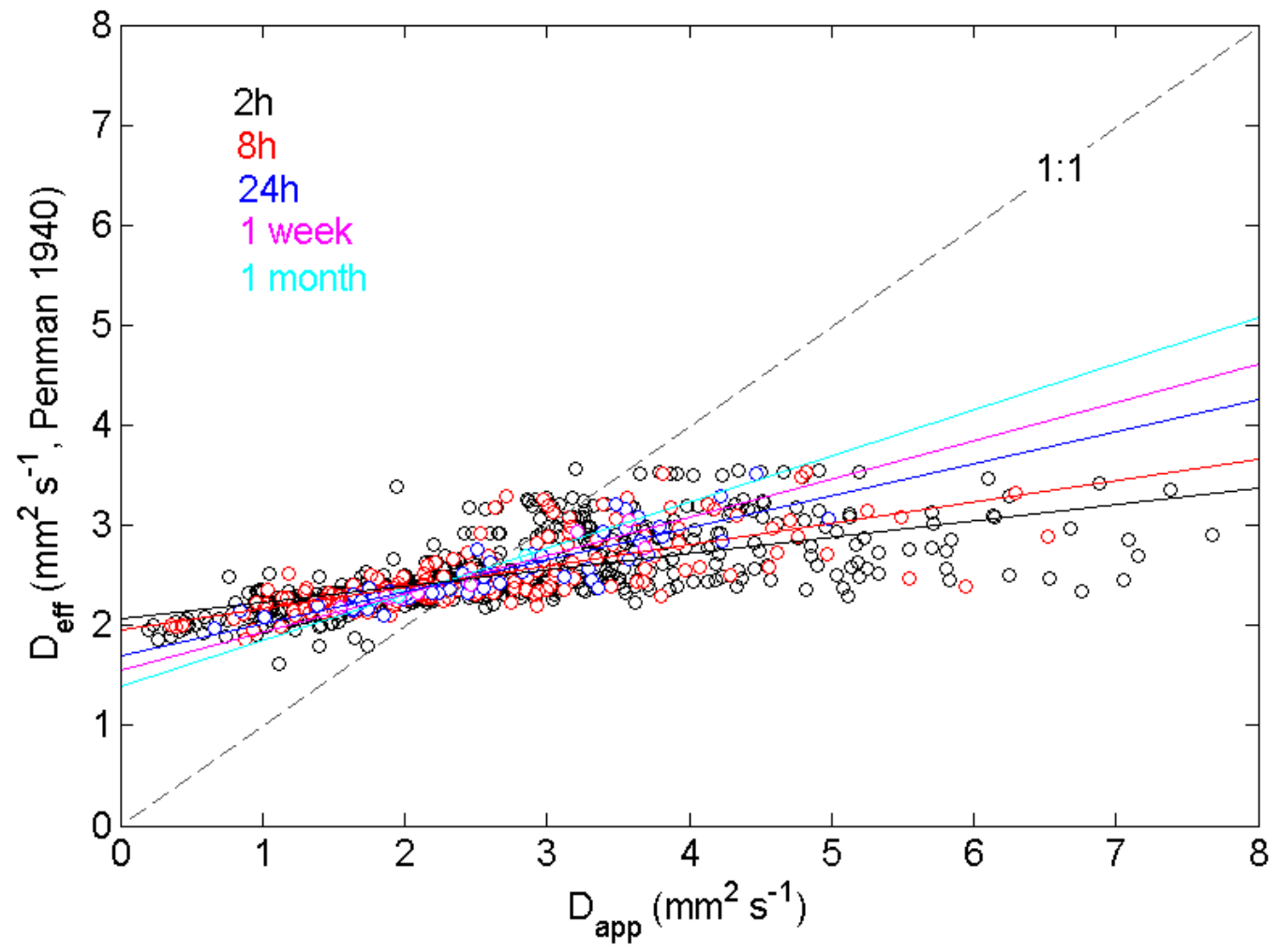


Figure 5

**Table 1**

Included parameters	% Variance in $D_{app}$ explained		
	All data	SWC<33%	SWC>33%
Wind, PAR, SWC	67	57	61
Wind, PAR	36	47	40

Table 1:

Multiple linear regression of wind speed, photosynthetically active radiation (PAR) and soil moisture content (SWC) with apparent diffusivity ( $D_{app}$ ), was used to calculate the percentage of variance in  $D_{app}$  explained by combinations of these three drivers. Regressions were carried out on the whole dataset, on the subset of data where SWC was below the threshold of 33% and on the subset of data where SWC was above this threshold.